Biomedical Engineering Letters (2023) 13:739–750
https://doi.org/10.1007/s13534-023-00296-6

ORIGINAL ARTICLE

Optimized deep neural network models for blood pressure classification using Fourier analysis-based time–frequency spectrogram of photoplethysmography signal

Pankaj[1] · Ashish Kumar[2] · Manjeet Kumar[3] · Rama Komaragiri[1]

Received: 17 February 2023 / Revised: 28 May 2023 / Accepted: 9 June 2023 / Published online: 24 June 2023

Abstract
Appropriate blood pressure (BP) management through continuous monitoring and rapid diagnosis helps to take preventive care against cardiovascular diseases (CVD). As hypertension is one of the leading causes of CVDs, keeping hypertension under control by a timely screening of subjects becomes lifesaving. This work proposes estimating BP from motion artifact-affected photoplethysmography signals (PPG) by applying signal processing techniques in realtime. This paper proposes a deep neural network-based methodology to accurately classify PPG signals using a Fourier theory-based time–frequency (TF) spectrogram. This work uses the Fourier decomposition method (FDM) to transform a PPG signal into a TF spectrogram. In the proposed work, the last three layers of the pre-trained deep neural network, namely, GoogleNet, DenseNet, and AlexNet, are modified and then used to classify the PPG signal into normotension, pre-hypertension, and hypertension. The proposed framework is trained and tested using the MIMIC-III and PPG–BP databases using five-fold training and testing. Out of the three deep neural networks, the proposed framework with the DenseNet-201 network performs best, with a test accuracy of 96.5%. The proposed work uses FDM to compute the TF spectrogram to accurately separate the motion artifacts and noise components from a noise-corrupted PPG signal. Capturing more frequency components that contain more information from PPG signals makes the deep neural networks extract better and more meaningful features. Thus, training a deep neural network model with clean PPG signal features improves the generalized capability of a BP classification model when tested in realtime.

Keywords Arterial blood pressure · Hypertension · Photoplethysmography · Fourier decomposition method · Time–frequency spectrogram · Deep learning · Transfer learning

1 Introduction

Continuous high blood pressure (BP) in a subject causes heart complications and increases the risk of heart attack and stroke. According to WHO reports [1], hypertension (HYP) is a major cause of untimely death. Around 1.28 billion in the age group of 30–79 years are affected by hypertension. Out of these, approximately 46% of adults are unaware they are suffering from hypertension [2]. Many do not receive the needed treatments because they feel no symptoms [3]. There is a known correlation between hypertension and cardiovascular diseases (CVD) [4]. CVD can be prevented through early diagnosis and control of hypertension. However, no proper and adequate means are available as the formation of HYP has no common or unified reasons. Only continuous BP monitoring and treatment can help to stabilize the BP at normal levels [5]. Reducing the frequency of HYP by 33%

✉ Manjeet Kumar
manjeetchhillar@gmail.com

Pankaj
er.pankaj08@gmail.com

Ashish Kumar
akumar.1june@gmail.com

Rama Komaragiri
rama.komaragiri@gmail.com

[1] Department of Electronics and Communication Engineering, Bennett University, Greater Noida, India

[2] School of Electronics Engineering, Vellore Institute of Technology, Chennai, Tamil Nadu, India

[3] Department of Electronics and Communication Engineering, Delhi Technological University, Delhi, India

up to 2030 is one of the global targets for non-communicable diseases [6].

In their daily routine, most people tend to ignore their health status due to many obligations. If a subject suffering from HYP fails to check the health status and is untreated, the risk of vision loss, stroke, heart failure, and other serious health problems increases significantly [7]. BP classification using a wearable device helps users know their BP condition timely and can provide an early warning system for potential patients. Thus, the research on the identification of HYP in real-time is increasing. Hence, the demand for reliable wearable healthcare devices that continuously monitor BP and promptly flag the BP state as normotension (NT), pre-hypertension (PH), or hypertension (HYP) is increasing.

During a heart cycle, when the heart pumps blood into the body, the pressure in the arteries is denoted by systolic BP (SBP). Diastolic BP (DBP) denotes the pressure in the arteries between heartbeats [8]. The oscillography and Korotkoff's sound method are commonly used to measure BP. These methods rely on building and releasing cuff pressure to detect SBP and DBP. However, the requirement of an arm cuff makes these techniques unsuitable for prolonged and continuous monitoring [9]. To continuously measure BP in realtime, the research is inclined toward designing wearable devices using PPG sensors [10]. The PPG technique uses a photo-electric sensor to extract the pulse wave signal due to blood volume changes during the systolic and diastolic phases [11].

During the systolic and diastolic phases, arterial blood pressure (ABP) depicts the pressure details of blood pumped out by the heart. Similarly, during a cardiac cycle, the PPG signal depicts a change in blood volume. Therefore, in recent years, the use of PPG signal to extract ABP signal information has emerged, as PPG signal has a high correlation with ABP in both time and frequency domains.

Accurate detection and early diagnosis of HYP are vital in preventing CVDs. In the past decade, the parameters extensively studied to estimate and classify BP are pulse transit time (PTT) and pulse wave velocity (PWV) [12].

Measuring PTT and PWV requires two sensors, thus having an increased system complexity. Further, PTT and PWV require calibration of sensors with different physiological conditions of subjects, thus unsuitable for real-time monitoring [13]. A pulse wave analysis (PWA) approach is proposed in [14] to classify BP by overcoming the need for two sensors.

Handcrafted features shown in Fig. 1 are extracted using PWA. These handcrafted features train a machine learning (ML) classification model [15]. In [16], an ML framework is trained using the first and second derivatives of a PPG signal and is proposed to classify BP. Training an ML model using handcrafted features is unreliable as these features vary significantly among subjects and are usually noise-sensitive. Also, the changes in the shape of PPG signals due to various diseases make it hard to extract the features accurately [17]. BP classification requires an accurate methodology that requires less or no intervention, making the ML-based models redundant for realtime BP classification in wearable devices. To overcome the person-specific morphological feature-based classification, deep learning-based BP classification approaches are recently becoming popular in the healthcare industry. The deep learning method consists end-to-end learning approach for BP classification. The end-to-end learning approach takes a 2-D image as input and captures the temporal and spectral information of a PPG signal. A deep neural network implicitly obtains features and correlates those features with actual values, allowing the network to perform better classification [18].

A two-class BP classification model is proposed using the cascade approach of CNN–LSTM [19]. A hybrid approach of CNN and the gated recurrent unit (GRU) for BP classification is proposed in [20]. A parallel convolutional layer network architecture is proposed to extract the features from PPG and ECG signals [21]. The studies mentioned above showed that acquiring PPG and ECG signals simultaneously is mandatory to achieve better accuracy and classify the BP using a deep neural network. The need for two sensor signals increases the system's complexity, which motivates single PPG sensor-based BP classification.

In [22], a pre-trained GoogLeNet deep neural network-based PPG signal classification is proposed. The reported work creates a PPG signal spectrogram using continuous

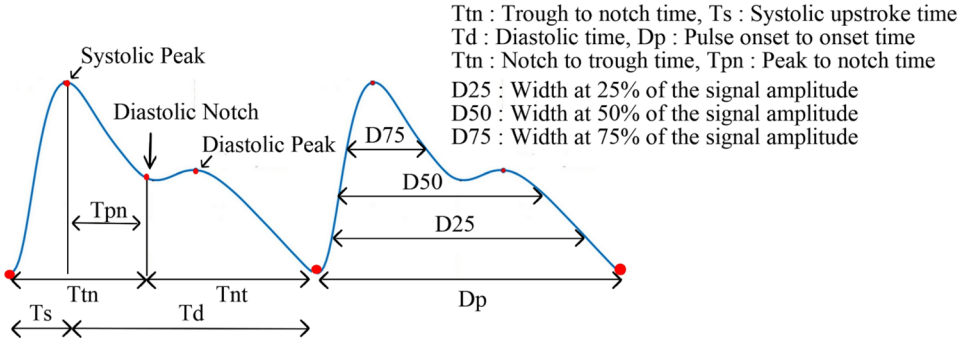

Fig. 1 Morphological features of PPG signal for BP estimation

wavelet transform (CWT) to train and test the GoogLeNet network. A CWT spectrogram and pre-trained deep neural network-based approach have been proposed [23]. In [24], a method based on wavelet transforms is proposed to improve the accuracy of the CNN model to predict and classify BP.

In [25], a hybrid LSTM-ANN model is proposed for BP classification using a PPG signal. In [26], a synchrosqueezing transform and a pre-trained deep neural network-based approach is proposed to classify BP automatically from a PPG signal. In [27], wavelet scattering transform (WST) and pre-trained neural network-based approach is proposed to classify the BP using PPG signal.

A convolutional neural network (CNN) model based on the mean impact value and genetic algorithm is proposed to desolate the statistical morphological-based process and predict the BP class [28]. The CNN and LSTM layer-based approach is proposed in [29]. The LSTM layer estimates the BP value based on the Eigenvalues extracted using the CNN layer. The work proposed in [30] introduced a multilayer perceptron neural network-based classification model to classify high blood pressure. A cascade approach of residual network CNN and bidirectional long short-term memory (BILSTM) is proposed to classify the BP into different classes [31]. This work obtains a high training accuracy but lacks test accuracy.

A 2-D convolutional neural network based on the Hilbert Huang Transform (HHT) framework is proposed to classify the BP state [32]. A personalized approach is applied to deep neural network transfer learning-based architecture to improve the classification accuracy of the model [33]. In [34], using various features of a PPG signal, a classifier is proposed to indicate the BP class.

The TF-based PPG signal analysis using a CNN-based model improves BP classification accuracy [35]. The method has a tradeoff in frequency resolution at high frequencies. Thus, exploring other TF analysis-based approaches for BP classification using a PPG signal is possible.

This work proposes a deep neural network-based classification methodology to classify three BP conditions: normotension (NT), pre-hypertension (PH), and hypertension (HYP). The proposed framework uses the potential of the Fourier decomposition method (FDM) to transform a 1-D PPG signal into a 2-D time–frequency (TF) spectrogram. The ability of the FDM method to provide fine spectral and temporal details of a non-stationary signal is used in this work to analyze the PPG signal.

The key highlights of the proposed work are given as follows.

(1) A Fourier series-based FDM technique is proposed for the first time to classify BP obtained using a PPG signal into multiclass.
(2) The FDM TF spectrogram decomposes the entire signal into a set of distinct frequency bands called Fourier intrinsic band functions (FIBFs), helping the model extract relevant features for accurate and reliable classification.
(3) This work investigates the performance of different pre-trained deep neural network models to differentiate between normal and hypertensive subjects based on PPG signal.
(4) The proposed work does not require additional ECG signals and manual PPG morphological feature extraction steps.

The organization of the rest of the paper is as follows. Section 2 describes the materials and methods of the proposed work. Section 3 presents the results obtained with the proposed framework, and Section 4 discusses a comparison with the state of art methods. Section 5 concludes the proposed work.

2 Material and methods

This section shows a detailed description of all blocks present in the proposed framework. A block diagram of the proposed work is shown in Fig. 2.

2.1 Data acquisition

The first stage of the proposed block diagram is related to the data collection stage. The multiparameter intelligent monitoring in intensive care (MIMIC-III) waveform database [36] is a publicly available dataset used in this work.

The MIMIC-III dataset contains multiple parameter recordings of more than 10,000 subjects.

The PPG and ABP signals are recorded at a sampling frequency of 125 Hz. A recording containing PPG and ABP signals is only considered for analysis.

The PPG signal is normalized using zero mean unit variance to get meaningful data. After normalization, the signal passes through the fourth-order Butterworth bandpass filter with a cutoff frequency [0.4–8] Hz. After filtering, the PPG signal is passed through the Hampel filtering stage to remove the outliers. The ABP signal is passed through the Hampel filtering stage to remove the outliers and then subjected to a peak detection algorithm to obtain true SBP and DBP values. The ABP signals are classified into NT, PH, and HYP BP labels, as per the seventh report of the Joint National Committee (JNC7).

The figshare dataset contains PPG signals acquired from 219 subjects aged between 21 and 86 years. The figshare database consists of a total of 657 PPG waveform segments. The dataset includes PPG, SBP, and DBP information from

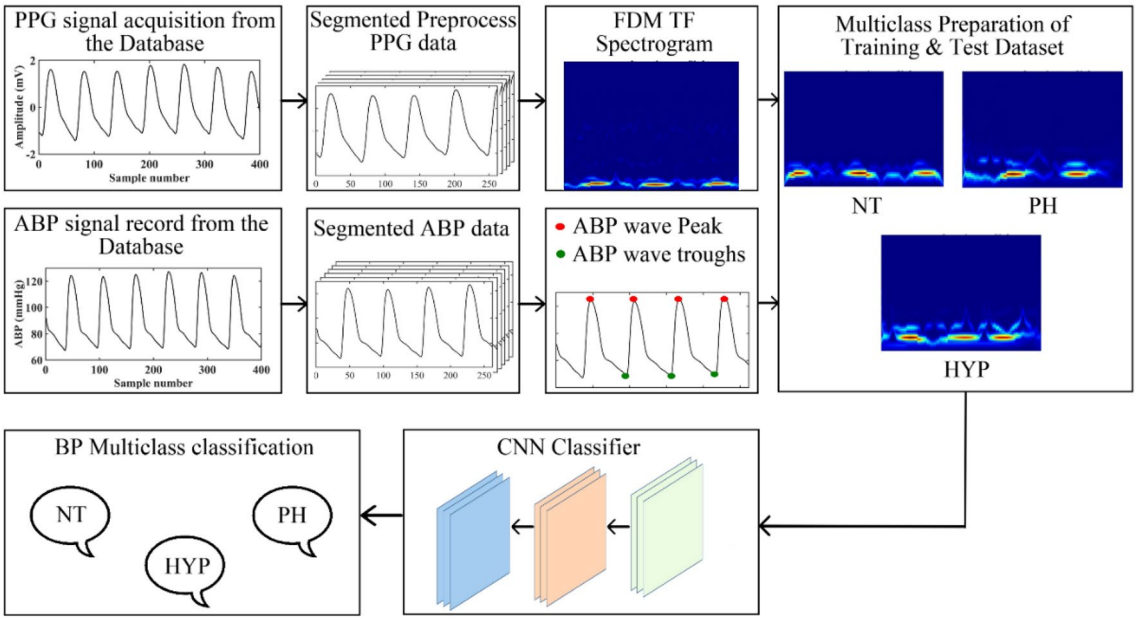

Fig. 2 Block diagram of the proposed method

the subjects diagnosed with NT, PHT, and HYP classes. The PPG signals are acquired in three segments per subject, each duration of 2.1 s. Each segment has 2100 samples at a sampling frequency of 1 kHz.

2.2 Mathematical background of Fourier decomposition method

FDM is a recently proposed valuable technique for analyzing non-stationary signals. FDM maps the sine and cosine basis function of the Fourier series into a finite number of band-limited analytic Fourier intrinsic band functions (FIBFs). The instantaneous frequencies of the FIBFs yield the TF distribution of any signal. Thus, FDM demonstrates its efficacy in analyzing non-stationary signals [37]. The FDM is an adaptive time-series method based on zero-phase filtering. FDM decomposes an input non-sinusoidal signal into a constant and a set of band-limited FIBFs. These energy-preserving FIBFs have a zero mean and are adaptive. FDM provides a clear time–frequency–energy (TFE) distribution of 1-D signal that discloses the time–frequency structure of the signal. The advantage of the FDM method is that it allows decomposing a signal into a desired number of FIBFs with varying amplitude and frequency in time [38].

Figure 3 shows the enhanced TFE representation of raw PPG signal indulged with noises and other undesired frequency components. The FDM method provides precise TFE analysis and effectively separates frequency bands during the signal decomposition, as shown in Fig. 3a.

The obtained FIBFs are adaptive and data-driven as a change in the input data changes these FIBFs. Each of the FIBFs obtained from the FDM contains a single frequency component.

The FDM-based TF is a 2-D graph representation of a 3-D spectrogram in which the amplitude (third dimension) is represented by color intensity. The spectrogram visually depicts the PPG signal strength over time at various frequencies present in the PPG waveform. The TF spectrogram represents the change in PPG signal amplitude over time. Along the horizontal axis in Fig. 3a, time runs from left to right. The vertical axis represents frequency, and the amplitude of a particular frequency at a particular time is represented using a color scale, with dark blues corresponding to low amplitudes and brighter colors up through red corresponding to progressively stronger amplitudes.

Figure 3b shows the FDM TF spectrogram of a preprocessed PPG signal divided into three different BP classes. The proposed method uses the 2-D TFE distribution as input to the pre-trained model.

2.3 Proposed methodology

The proposed framework is shown in Fig. 2. A PPG signal collected from the MIMIC database is first segmented into a consecutive window of 2.1 s. This segmentation process increases the number of PPG-BP categories of NT, PH, and HYP. After segmentation, each 2.1-s window is passed through the FDM block to compute a 2-D TF spectrogram. In the proposed framework, 2181 2-D TF spectrogram

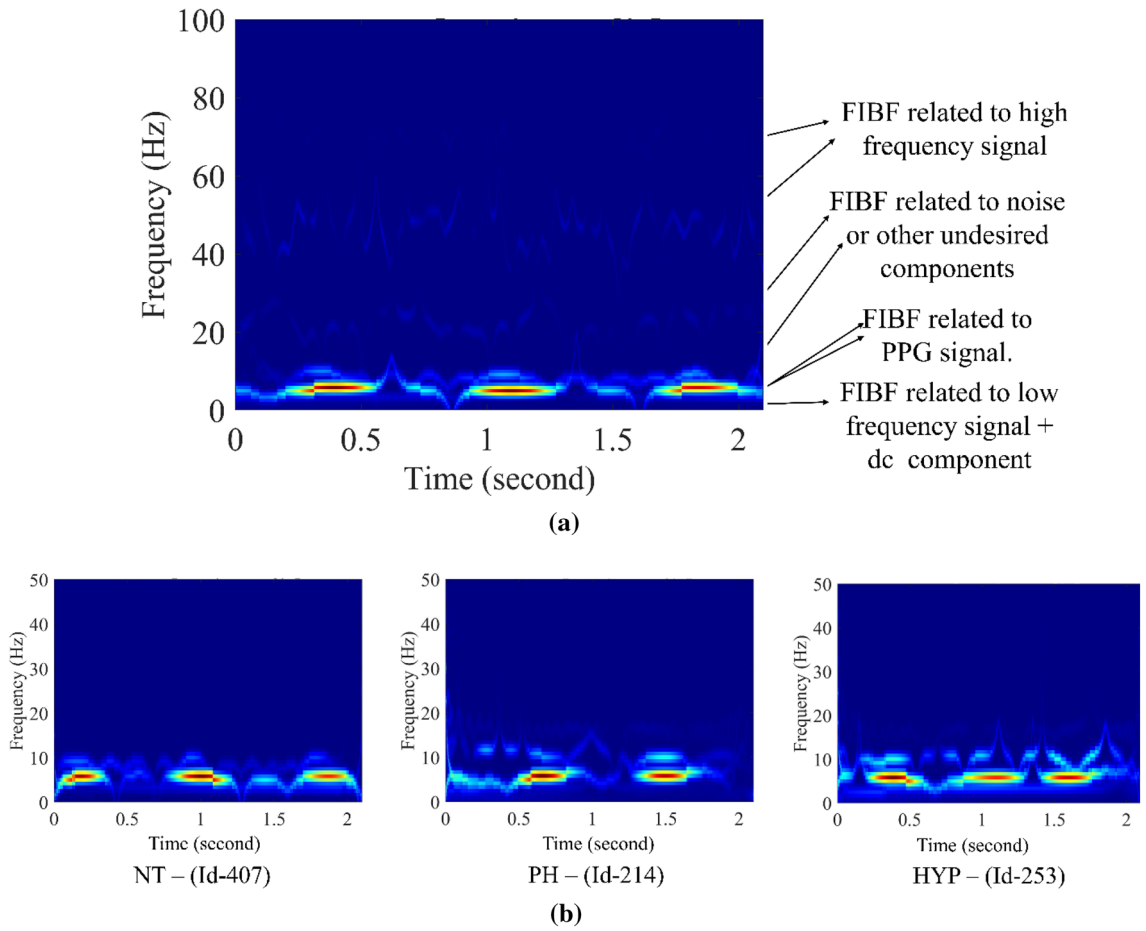

Fig. 3 **a** TFE representation of a PPG signal obtained using FDM, 3 **b** The FDM TF spectrogram cases of the three different BP categories. (Color figure online)

Table 1 JNC7 guidelines for BP classification

Classification type	SBP (mmHg)		DBP (mmHg)
NT	< 120	And	< 80
PH	120–139	Or	80–89
HYP	> 140	Or	> 90

images are obtained using the FDM algorithm belonging to NT, PH, and HYP classes.

ABP signals are segmented into the same window duration to label the BP levels and analyze the accuracy of the classifier. Table 1 lists the BP classes as per the American College of Cardiology/American Heart Association (ACC/AHA) 2017 Hypertension Guidelines [39].

For an ABP window, the mean of all synchronous wave peaks shown by the red dots in Fig. 2 are used to calculate SBP. The mean of the synchronous wave trough shown by the green dots are used to calculate the DBP.

In the proposed framework, each BP class has 650 images, out of which 97 are used to validate the classifier. A set of 231 images consisting of 77 images from each class are used to test the classifier. This work introduces the pre-trained deep neural network model to classify the PPG signal. Three neurons in the last fully connected layer classify BP into three classes. Parameters like initial learning rate, validation frequency, solver, batch size, and learning rate drop factor of the classifier are optimized to obtain the best classification accuracy.

2.4 Deep neural network classifier

Transfer learning is one of the important aspects of a deep neural network. The deep neural network is initially trained on a larger image dataset in transfer learning. These pre-trained deep networks can be used directly to classify thousands of categories. The strong in-depth characteristics of a pre-trained model allow network generalization by transfer learning [40].

Thus, transfer learning can be used for many applications if the input signal to the model is of type 2-D images. In this work, the updated weight of the pre-trained network is transferred to classify the new dataset. GoogLeNet, DenseNet, and AlexNet deep neural networks are fine-tuned and trained based on the MIMIC-III dataset to solve the problem of BP multiclass classification.

GoogLeNet is a pre-trained CNN framework variant of the Inception architecture [41]. Input to the GoogLeNet is a $224 \times 224 \times 3$ sized 2-D image. In this work, the GoogLeNet architecture uses a dropout layer with a dropout factor of 0.4 to prevent the model from overfitting during training.

DenseNet is a pre-trained neural network in which each layer is connected to every layer except itself, thus also called a Densely connected neural network [42]. For an L-layer DenseNet network, there are $L\ (L+1)/2$ direct connections. In DenseNet, the feature map obtained with $(L-1)th$ layer is fed as input to the Lth layer. The feature map of the Lth layer is fed as an input for each subsequent layer. DenseNet-201 [43] is a version of DenseNet used in the proposed work to classify the PPG signals.

AlexNet consists of eight layers; the first five are convolutional layers. The remaining three are fully connected layers. The AlexNet has an average pooling and rectified linear unit (ReLU) layer between two consecutive convolutional layers [44]. The use of the ReLU layer makes the model learning process faster. The output of the last fully connected layer is passed through the activation function softmax to predict the class of the input images.

3 Result analysis

3.1 Performance metrics

The metrics used to check the performance of the proposed framework are accuracy, specificity, precision, sensitivity, and F1-score, shown in Eq. (1). These metrics are estimated by using true positives (TP), false positives (FP), true negatives (TN), and false negatives (FN).

$$\begin{aligned} Accuracy &= \frac{TP+TN}{TP+TN+FP+FN} \times 100 \\ Specificity &= \frac{TN}{TN+FP} \times 100 \\ precision &= \frac{TP}{TP+FP} \times 100 \\ Sensitivity &= \frac{TP}{TP+FN} \times 100 \\ F1-Score &= \frac{2 \times precision \times sensitivity}{precision + sensitivity} \end{aligned} \tag{1}$$

3.2 Simulation results

The pre-trained neural network automatically extracts features from the input 2-D TF spectrogram. The pre-trained neural network correlates different classes with the extracted features to recognize the class when a new dataset (test dataset) is fed as an input to the network. This work compares the performance of the three pre-trained neural networks, GoogleNet, DenseNet, and AlexNet, to classify BP into three classes. The pre-trained GoogLeNet architecture with 144 layers is trained to classify the PPG records in the proposed method. The last three layers in the GoogLeNet architecture are replaced to categorize the new images. The input PPG spectrogram is resized to 224×224 to fulfill the input image size requirement of the GoogLeNet. An initial learning rate of 0.001 with a batch size of 40 and validation frequency of 40 is fixed for this work. The GoogLeNet resulted in 94.92% training accuracy and 94.81% testing accuracy. Figure 4 shows the confusion matrix for the training and test dataset.

The DenseNet-201 pre-trained neural network is used for BP classification. The input PPG spectrogram is resized to 224×224 to fulfill the input image size requirement of the DenseNet-201. The parameter of the last three layers is optimized to recognize the three PPG signal classes. An initial learning rate of 0.001 with a batch size of 40 and Adam optimizer are used to train the proposed DenseNet-201 network. The DenseNet resulted in 96.92% training accuracy and 96.51% testing accuracy. Figure 5 shows the confusion matrix for the training and test datasets.

In the AlexNet network, the input spectrograms are resized to $227 \times 227 \times 3$. In this proposed work, the parameters of the last three layers are optimized to obtain the best results. Adam optimizer trains the AlexNet model with an initial learning rate of 0.001 and a batch size of 40. A validation frequency of 40 is fixed for this work. The AlexNet resulted in 95.51% training accuracy and 95.21% testing accuracy. Figure 6 shows the confusion matrix for the training and test dataset.

To analyze the performance of this work, the performance metrics (Accuracy, precision, sensitivity, specificity, and F-1 score) are calculated from the training and test datasets. Tables 2, 3 and 4 show the performance analysis of GoogleNet, DenseNet-201, and AlexNet on the test dataset and demonstrate the potential of the proposed FDM-TF-based classification.

The proposed FDM-TF-based method is compared with various works from the literature. For a fair comparison, three classification experiments are examined from the confusion matrix: NT versus PH, NT versus HYP, and NT + PH versus HYP. The F1-score obtained for NT versus PH, NT versus HYP, and NT + PH versus HYP with the proposed work using GoogLeNet, DenseNet-201 and for AlexNet are shown in Tables 2, 3 and 4.

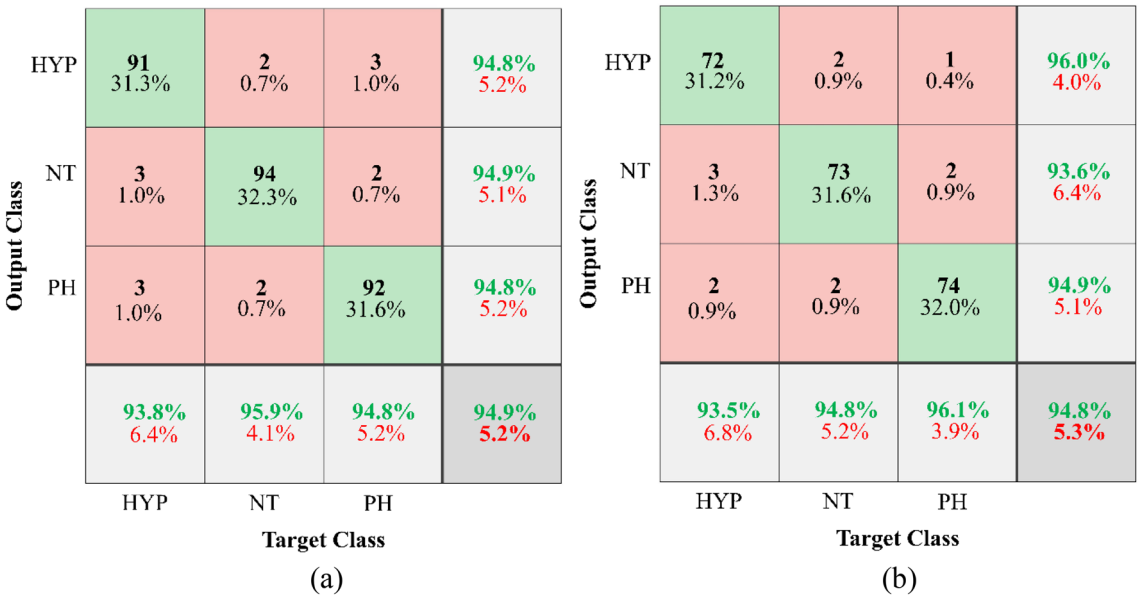

Fig. 4 Confusion matrix of the **a** training dataset and **b** the testing dataset obtained using GoogLeNet

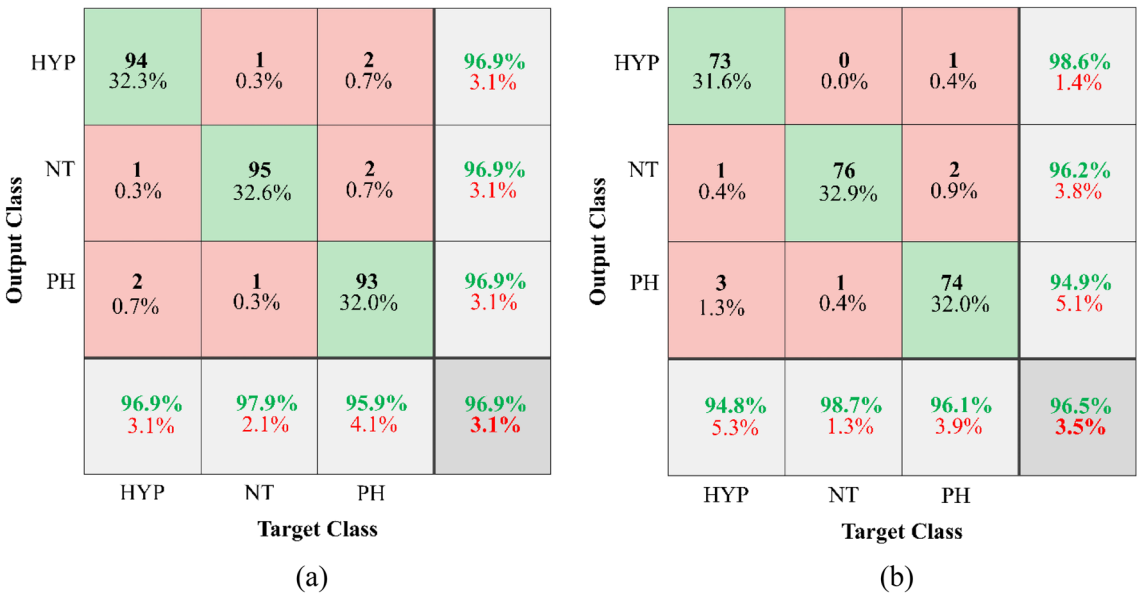

Fig. 5 Confusion matrix of the **a** training dataset and **b** the testing dataset obtained using DenseNet-201

Out of the three deep neural networks, the DenseNet-201 and AlexNet performed better than the GoogLeNet model. Thus, we tested both models further using the figshare dataset. The F1-score obtained using DenseNet-201 for NT versus PH, NT versus HYP, and NT + PH versus HYP is 98.06, 99.34 and 97.40 respectively. The AlexNet obtained a F1-score for NT versus PH, NT versus HYP, and NT + PH versus HYP is 97.61, 98.15 and 96.80 respectively. The F1-score is higher for the proposed FDM-TF-based method tested using Densenet-201.

A fivefold cross-validation approach is used for better utilization of the dataset and to improve the robustness of the optimized deep neural network model. The model performance is evaluated five times, where each fold out of fivefold acts as a test dataset, and the remaining four folds are fed to train the model. The final performance of the model is evaluated by averaging the accuracy obtained in all five trials.

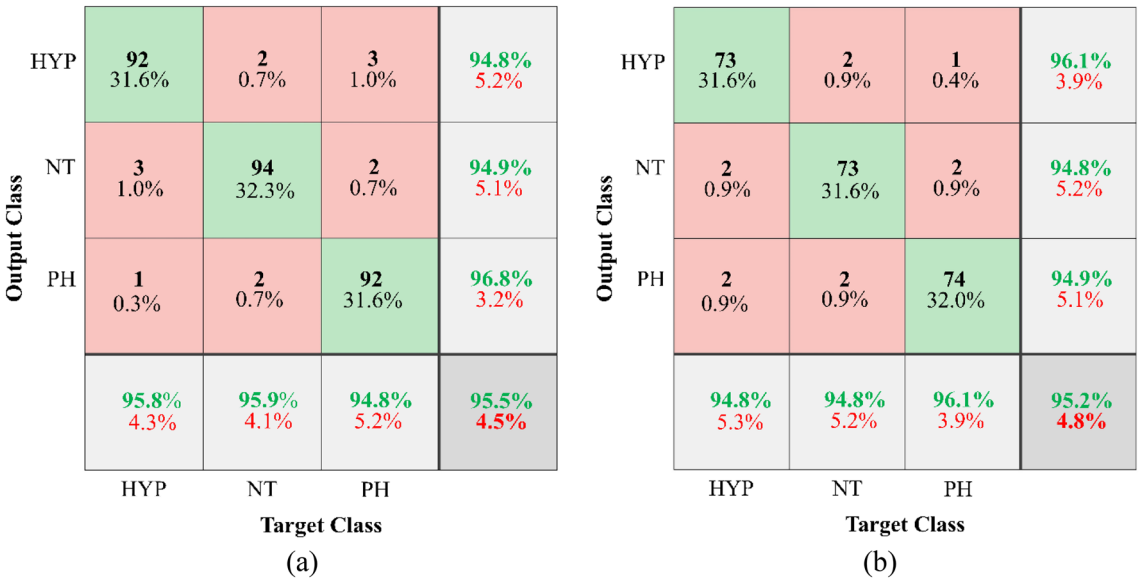

Fig.6 Confusion matrix of the **a** training dataset and **b** the testing dataset obtained using AlexNet

Table 2 Performance Analysis of FDM TF method using GoogLeNet

	TP	FP	FN	TN	Accuracy	Precision	Sensitivity	Specificity	F1-Score
HYP	72	5	3	147	96.47	93.5	96	96.71	94.73
NT	73	4	5	146	96.05	94.8	93.58	97.33	94.19
PH	74	3	4	145	96.9	96.1	94.87	97.97	95.48
NT versus PH	73	2	2	74	97.35	97.33	97.33	97.36	97.33
NT versus HYP	73	2	3	72	96.67	97.33	96.05	97.29	96.68
(NT + PH) versus HYP	147	3	9	72	94.8	98	94.23	96	96.07

Table 3 Performance analysis of FDM TF method using DenseNet-201

	TP	FP	FN	TN	Accuracy	Precision	Sensitivity	Specificity	F1-Score
HYP	73	4	1	150	97.8	94.8	98.64	97.4	96.68
NT	76	1	3	147	98.23	98.7	96.2	99.32	97.43
PH	74	3	4	149	96.95	96.1	94.87	98.02	95.48
NT versus PH	76	1	2	74	98.03	98.7	97.43	98.67	98.06
NT versus HYP	76	0	1	73	99.33	100	98.7	100	99.34
(NT + PH) versus HYP	150	1	7	73	96.53	99.33	95.54	98.64	97.4

Table 4 Performance analysis of FDM TF method using AlexNet

	TP	FP	FN	TN	Accuracy	Precision	Sensitivity	Specificity	F1-Score
HYP	73	4	3	147	96.91	94.8	96.05	97.35	95.42
NT	73	4	4	147	96.49	94.8	94.8	97.35	94.8
PH	74	3	4	146	96.91	96.1	94.87	97.98	95.48
NT versus PH	73	2	2	74	97.35	97.33	97.33	97.36	97.33
NT versus HYP	73	2	2	73	97.33	97.33	97.33	97.33	97.33
(NT + PH) versus HYP	147	3	8	73	95.23	98	94.83	96.05	96.39

The average test accuracy of the proposed framework with fivefold cross-validation using GoogLeNet, DenseNet, and AlexNet is 95.12%, 96.71%, and 95.28%, respectively. These results are similar to accuracy values obtained without using the fivefold cross-validation approach shown in Figs. 4, 5 and 6.

Table 5 compares the overall accuracy obtained with the optimized pre-trained neural network with other existing methods. The results indicate that BP classification using DenseNet + FDM achieves better accuracy than the methods listed in Table 5.

4 Discussion

The proposed method has the potential to detect the BP level in realtime accurately. This method only uses a raw PPG signal and replaces the cuff-base and PPG morphology feature extraction process for BP classification.

This paper presents an optimized deep neural network framework to classify the BP into multiple classes: NT, PH, and HYP. The proposed framework explores the potential of the FDM TF spectrogram to classify BP in realtime only by using a PPG signal. The acquired 1-D PPG signal is transformed into a 2-D TF spectrogram using the FDM method. FDM decomposes the acquired preprocessed PPG signal into desirable FIBF with varying amplitude and frequency with time. FDM provides better TF estimation and separates FIBFs related to the clean and noise signals.

In recent times, with the introduction of artificial intelligence, the estimation and classification of BP using wearable devices have emerged. BP classification using a wearable device helps the user to know their BP condition timely and acts as an early warning system.

Therefore, this work used FDM based TF spectrogram of PPG signals to train and test the deep neural network to accurately classify PPG signals into three BP classes per the criterion given by ACC/AHA hypertension guidelines 2017.

The proposed framework demonstrated a classification accuracy of BP in multiclass for three optimized pre-trained deep neural network models trained and tested using MIMIC-III and figshare datasets. The proposed framework obtained 95.12%, 96.71%, and 95.28% accuracy for GoogLeNet, DenseNet, and AlexNet, respectively.

The work proposed in [16] shows a significant performance with an F1-score of 97.51% for the classification of NT versus HYP. However, the performance of the framework report in [16] requires first derivative PPG and second derivative PPG in addition to the PPG signal for model training. The work reported in [49] shows significant results compared to the proposed work. However, the performance of this work relies on the feature value extracted manually from the TF spectrogram of the PPG signal. The value of the features strongly depends on the morphological structure of the PPG signal, which can change due to noise and disease. The work proposed in [21] obtained an accuracy of 95% for classifying BP in five classes. However, this work concatenates the feature extracted from the PPG and ECG signals. Thus, the need for the PPG signal and the ECG signal for feature extraction increases the computational complexity of the system.

Most of the techniques in the literature require an additional PPG sensor or an ECG signal to extract features from the PPG signal to train the machine-learning model. Thus,

Table 5 Performance comparison of the proposed work with the existing work

Author	Method	Number of classes	Overall accuracy (%)
LaFreniere et al. 2017 [45]	Feedforward neural network	2	82.00
Patnaik et al. 2018 [46]	Support vector machine	2	80.23
Luo et al. 2018 [47]	CNN	2	89.95
Fitriyani et al. 2019 [48]	Ensemble machine learning model	2	85.73
Tjahjadi et al. 2020 [49]	Bidirectional long short-term memory + CWT	3	93.00
Wu et al. 2021 [24]	CNN + CWT	2	90.36
Wu et al. 2021 [24]	GoogLeNet + CWT	2	84.54
Yen et al. 2021 [31]	ResNetCNN + BiLSTM	4	76%
Fuadah et al. 2022 [21]	Concatenated 1-D CNN	5	95%
Kuzmanov et al. 2022 [20]	ECG + PPG	3	78%
Martinez et al. 2022 [50]	WST + SVM	2	71.4%
Zhang et al. 2023 [51]	STFT + CNN	2	75%
Proposed work	GoogLeNet + FDM	3	95.12
Proposed work	DenseNet-201 + FDM	3	96.71
Proposed work	AlexNet + FDM	3	95.28

the performance of these techniques relies on the requirement of two signals. Moreover, the synchronization between the two signals in realtime is challenging.

The work proposed in [32] shows a comparable performance for NT versus PH classification, but the reported work does not provide good results for other classification types. The performance of the reported work [32] depends on the feature extracted from three signals (PPG, first derivative PPG, and second derivative PPG signal).

Further, the main hurdle associated with realtime acquired PPG signal is the effect of motion artifacts which degrade the algorithm's accuracy. Thus, removing motion artifact components from a PPG signal is also a factor to consider while designing a wearable device. Most of the work reported in the literature used features extracted from a raw PPG signal to train and test the model. Training a machine learning model with features acquired from the corrupted PPG signal reduces the generalized capability of the model when tested in realtime, as the effect of motion artifacts is random. Notably, a deep neural network has the potential to automatically extract relevant features and map these features with the target class. It is assumed that training a model with a corrupted PPG signal consisting of random and irregular peaks degrades the generalized capability of the model when tested in realtime. Thus, the proposed work trains the deep neural network model using an FDM-based TF spectrogram to increase the model's accuracy.

The parameters of the pre-trained neural network are optimized to improve the accuracy of the classifier. The model accuracy on the test dataset is evaluated using the performance metrics accuracy, specificity, sensitivity, precision, and the F1-score.

5 Conclusion and future scope

A deep learning-based approach to analyzing PPG signals helps improve classification accuracy. The proposed study is tested using publicly available MIMIC-III and figshare datasets. A new framework by combining FDM-based TF spectrogram and deep neural network architectures is proposed so that the same can be used in smart wearable healthcare devices for early diagnosis of hypertension to reduce the mortality rate.

This work uses PPG signals from the MIMIC-III database as an input to produce a 2-D TF spectrogram from a 1-D PPG input signal by applying FDM. The obtained TF spectrogram is used as an input image database of the pre-trained deep neural network. FDM TF spectrogram accurately separates the motion artifacts and other unwanted frequency components from the PPG signal. Thus, the model training becomes more robust and accurate. This work considered three pre-trained deep neural networks: GoogLeNet, DenseNet, and AlexNet. In this work, the parameter of the last three layers of the pre-trained network are optimized to meet the classification needs. Out of the three pre-trained networks used in this work, the DenseNet-201 provides the highest classification accuracy of 96.71%. The confusion matrix shows the potential of DenseNet-201 to successfully classify the PPG spectrogram into multiclass (NT, PH, and HYP). For BP classification, each class is equally important to provide the BP state of a user in realtime. Thus, the overall performance of the classifier is measured using the F1-score that combines precision and recall. A high F1 score indicates the model's efficiency in accurately classifying BP. After analysis of computational time taken by all proposed deep neural network, it is found that DenseNet-201 training time, testing time, and model complexity is higher than the GoogLeNet and AlexNet. Although DenseNet-201 provides better accuracy than the AlexNet and the GoogLeNet, indicating that there is a tradeoff between system complexity and system performance.

This work is performed over a non-GPU device; thus, the training and testing time are high. For future studies, we plan to increase the dataset and train and test the pre-trained model on a GPU-based workstation.

Author contributions P: Conceptualization, Methodology, Software, Data Curation, Investigation, Writing—Original draft preparation. AK: Conceptualization, Investigation, Visualization, Writing-Reviewing and Editing, Supervision. MK: Investigation, Visualization, Writing-Reviewing and Editing, Supervision. RK: Investigation, Visualization, Writing-Reviewing and Editing, Supervision.

Funding No funding Received.

Declarations

Conflict of interest All Authors of this work declare no conflict of interest.

Ethical approval This article does not contain any studies with human participants or animals performed by any of the authors.

References

1. Health topic, cardiovascular disease, world health organization. 2023. https://www.who.int/health-topics/hypertension. Accessed 31 Mar 2023.
2. Hypertension, key facts, world health organization. 2023. https://www.who.int/news-room/fact-sheets/detail/hypertension. Accessed 31 Mar 2023.
3. Meyerovitz CV, et al. Social determinants, blood pressure control, and racial inequities in childbearing age women with hypertension, 2001 to 2018. J Am Heart Assoc. 2023;12(5):e027169.
4. Fuchs FD, Whelton PK. High blood pressure and cardiovascular disease. Hypertension. 2020;75:285–92.

5. Song K, Chung KY, Chang JH. Cuffless deep learning-based blood pressure estimation for smart wristwatches. IEEE Trans Instrum Meas. 2020;69(7):4292–302.
6. Al-Makki A, et al. Hypertension pharmacological treatment in adults: a world health organization guideline executive summary. Hypertension. 2022;79(1):293–301.
7. Haghi M, Thurow K, Stoll R. Wearable devices in medical internet of things: scientific research and commercially available devices. Healthc Inform Res. 2017;23(1):4–15.
8. Pankaj, Kumar A, Komaragiri R, Kumar M. A review on computation methods used in photoplethysmography signal analysis for heart rate estimation. Arch Comput Methods Eng. 2022;29(2):921–40.
9. Kachuee M, Kiani MM, Mohammadzade H, Shabany M. Cuffless blood pressure estimation algorithms for continuous healthcare monitoring. IEEE Trans Biomed Eng. 2017;64(4):859–69.
10. Kumar A, Ashdhir A, Komaragiri R, Kumar M. Analysis of photoplethysmogram signal to estimate heart rate during physical activity using fractional Fourier transform–a sampling frequency independent and reference signal-less method. Comput Methods Programs Biomed. 2023;229:107294.
11. Pankaj, Kumar A, Kumar M, Komaragiri R. STSR: spectro-temporal super-resolution analysis of a reference signal less photoplethysmogram for heart rate estimation during physical activity. IEEE Trans Instrum Meas. 2022;71:1–10.
12. Esmaelpoor J, Moradi MH, Kadkhodamohammadi A. A multistage deep neural network model for blood pressure estimation using photoplethysmogram signals. Comput Biol Med. 2020;120:103719.
13. Li Z, He W. A continuous blood pressure estimation method using photoplethysmography by GRNN-based model. Sensors. 2021;21(21):7207.
14. Teng XF, Zhang YT Continuous and noninvasive estimation of arterial blood pressure using a photoplethysmographic approach. 2003. pp. 3153–3156
15. Tjahjadi H, Ramli K. Noninvasive blood pressure classification based on photoplethysmography using K-nearest neighbors algorithm: a feasibility study. Information (Switz). 2020;11(2):93.
16. Hu X, et al. Blood pressure stratification using photoplethysmography and light gradient boosting machine. Front Physiol. 2023;14:231.
17. Evdochim L, Dobrescu D, Halichidis S, Dobrescu L, Stanciu S. Hypertension detection based on photoplethysmography signal morphology and machine learning techniques. Appl Sci (Switz). 2022;12(16):8380.
18. Schrumpf F, Frenzel P, Aust C, Osterhoff G, Fuchs M. Assessment of non-invasive blood pressure prediction from PPG and RPPG signals using deep learning. Sensors. 2021;21(18):6022.
19. Kuzmanov I, Bogdanova AM, Kostoska M, Ackovska N Fast cuffless blood pressure classification with ECG and PPG signals using CNN–LSTM models in emergency medicine. In: 2022 45th Jubilee international convention on information, communication and electronic technology (MIPRO). 2022; pp. 362–7.
20. Kuzmanov I, Kostoska M, Bogdanova AM. Blood pressure class estimation using CNN-GRU model. In: 2022 The 19th International Conference on Informatics and Information Technologies, CIIT 2022. In 2021 IEEE Computing in Cardiology, CinC 2021. 2021;Vol. 48; pp. 1–4.
21. Fuadah YN, Lim KM. Classification of blood pressure levels based on photoplethysmogram and electrocardiogram signals with a concatenated convolutional neural network. Diagnostics. 2022;12(11):2886.
22. Liang Y, Chen Z, Ward R. Photoplethysmography and deep learning: enhancing hypertension risk stratification. Biosensors. 2018;8:101.
23. Cano J, Bertomeu-González V, Fácia L, Zangróniz R, Alcaraz R, Rieta JJ. Hypertension risk assessment from photoplethysmographic recordings using deep learning classifiers.
24. Wu J, Liang H, Ding C, Huang X, Huang J, Peng Q. Improving the accuracy in classification of blood pressure from photoplethysmography using continuous wavelet transform and deep learning. Int J Hypertens. 2021;9938584:2021.
25. Faris Ali N, Atef M. An efficient hybrid LSTM-ANN joint classification-regression model for PPG based blood pressure monitoring. Biomed Signal Process Control. 2023;84:104782.
26. Tanc YH, Ozturk M. Hypertension classification using PPG signals. In: 2022 medical technologies congress (TIPTEKNO). IEEE; 2022. pp. 1–4.
27. Martinez-Ríos EA, Montesinos L, Alfaro M. A comparison between wavelet scattering transform and transfer learning for elevated blood pressure detection. In: 2022 BMEiCON. IEEE; 2022. pp. 1–5.
28. Tanveer MS, Hasan MK. Cuffless blood pressure estimation from electrocardiogram and photoplethysmogram using waveform based ANN-LSTM network. Biomed Signal Process Control. 2019;51:382–92.
29. Tazarv A, Levorato M. A deep learning approach to predict blood pressure from PPG signals. In 2021 IEEE 43rd Annual international conference of the IEEE engineering in medicine & biology society (EMBC), 2021;pp. 5658–5662.
30. Kwong EWY, Wu H, Pang GKH. A prediction model of blood pressure for telemedicine. Health Inform J. 2018;24(3):227–44.
31. Yen CT, Chang SN, Liao CH. Deep learning algorithm evaluation of hypertension classification in less photoplethysmography signals conditions. Meas Control (UK). 2021;54(3–4):439–45.
32. Sun X, Zhou L, Chang S, Liu Z. Using CNN and HHT to predict blood pressure level based on photoplethysmography and its derivatives. Biosensors (Basel). 2021;11(4):120.
33. Schrumpf F, Serdack PR, Fuchs M. Regression or classification? Reflection on BP prediction from PPG data using deep neural networks in the scope of practical applications. In: 2022 Proceedings of the IEEE/CVF Conference on Computer Vision and Pattern Recognition, 2022; pp. 2172–2181
34. Riaz F, Azad MA, Arshad J, Imran M, Hassan A, Rehman S. Pervasive blood pressure monitoring using Photoplethysmogram (PPG) sensor. Futur Gener Comput Syst. 2019;98:120–30.
35. Mansouri SR, Lowe A, Gholamhosseini H, Baig MM. Blood pressure estimation from electrocardiogram and photoplethysmography signals using continuous wavelet transform and convolutional neural network. Conf-Irm 2019, 28;2019. https://aisel.aisnet.org/confirm2019/28
36. Johnson AEW, et al. Data descriptor: MIMIC-III, a freely accessible critical care database. Scientific data 2016;3(1):1–9.
37. Singh P, Joshi SD, Patney RK, Saha K. The Fourier decomposition method for nonlinear and non-stationary time series analysis. Proc R Soc A Math Phys Eng Sci. 2017;473(2199):20160871.
38. Pankaj, Kumar A, Komaragiri R, Kumar M. Reference signal less Fourier analysis based motion artifact removal algorithm for wearable photoplethysmography devices to estimate heart rate during physical exercises. Comput Biol Med. 2022;141:105081.
39. Whelton PK, et al. 2017 ACC/AHA/AAPA/ABC/ACPM/AGS/APhA/ASH/ASPC/NMA/PCNA guideline for the prevention, detection, evaluation, and management of high blood pressure in adults: a report of the American College of Cardiology/American Heart Association task force on clinical practice guidelines. J Am Coll Cardiol. 2018;71(19):e127–248.
40. Alzubaidi L, et al. Review of deep learning: concepts, CNN architectures, challenges, applications, future directions. J Big Data. 2021;8(1):1–74.
41. Szegedy C, et al. Going deeper with convolutions. Sep. 2014, Online. Available at http://arxiv.org/abs/1409.4842

42. Huang G, Liu Z, van der Maaten L, Weinberger KQ. Densely connected convolutional networks. Aug. 2016, [Online]. Available at http://arxiv.org/abs/1608.06993
43. Li T, Jiao W, Wang LN, Zhong G. Automatic DenseNet sparsification. IEEE Access. 2020;8:62561–71.
44. Krizhevsky A, Sutskever I, Hinton GE. ImageNet classification with deep convolutional neural networks. [Online]. Available at http://code.google.com/p/cuda-convnet/
45. Lafreniere D, Zulkernine F, Barber D, Martin K. Using machine learning to predict hypertension from a clinical dataset. In: 2016 IEEE symposium series on computational intelligence, SSCI 2016, 2017.
46. Patnaik R, Chandran M, Lee SC, Gupta A, Kim C. Predicting the occurrence of essential hypertension using annual health records. In: 2018 2nd International Conference on Advances in Electronics, Computers and Communications, ICAECC 2018; vol. 13, pp. 1–5:2018.
47. Luo Y, Li Y, Lu Y, Lin S, Liu X. The prediction of hypertension based on convolution neural network. In: 2018 IEEE 4th international conference on computer and communications, ICCC 2018. pp. 2122–2127;2018.
48. Fitriyani NL, Syafrudin M, Alfian G, Rhee J. Development of disease prediction model based on ensemble learning approach for diabetes and hypertension. IEEE Access. 2019;7:144777–89.
49. Tjahjadi H, Ramli K, Murfi H. Noninvasive classification of blood pressure based on photoplethysmography signals using bidirectional long short-term memory and time-frequency analysis. IEEE Access. 2020;8:20735–48.
50. Martinez-Ríos E, Montesinos L, Alfaro-Ponce M. A machine learning approach for hypertension detection based on photoplethysmography and clinical data. Comput Biol Med. 2022;145:105479.
51. Zhang C, et al. Video based cocktail causal container for blood pressure classification and blood glucose prediction. IEEE J Biomed Health Inform. 2023;27(2):1118–28.